

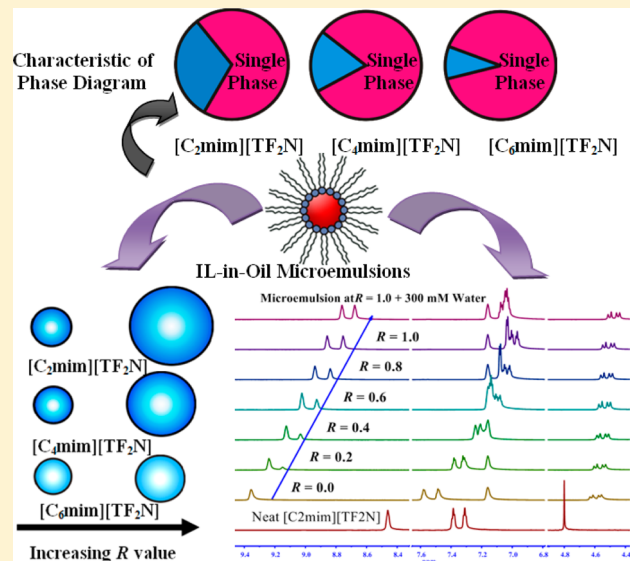
Phase Boundaries, Structural Characteristics, and NMR Spectra of Ionic Liquid-in-Oil Microemulsions Containing Double Chain Surface Active Ionic Liquid: A Comparative Study

Vishal Govind Rao, Sarthak Mandal, Surajit Ghosh, Chiranjib Banerjee, and Nilmoni Sarkar*

Department of Chemistry, Indian Institute of Technology, Kharagpur 721302, WB, India

Supporting Information

ABSTRACT: A method developed for the first time, to create a huge number of ionic liquid (IL)-in-oil microemulsions has been discussed in our earlier publication (Rao, V. G.; Ghosh, S.; Ghatak, C.; Mandal, S.; Brahmachari, U.; Sarkar, N. *J. Phys. Chem. B* 2012, 116, 2850–2855). Here, we present facile methods to adjust the structural parameters of microemulsions using different ionic liquids (ILs) as additives (polar phase). We have characterized ILs/[C₄mim][AOT]/benzene ternary system by performing a phase behavior study, dynamic light scattering (DLS) measurements, and ¹H NMR measurements. The IL loading capacity of microemulsions (area of single phase region) (i) increases with increase in alkyl chain length of cation of ILs and follows the trend [C₆mim][TF₂N] > [C₄mim][TF₂N] > [C₂mim][TF₂N], (ii) increases with decrease in cation anion interaction strength of added ILs and follows the trend [C₄mim][TF₂N] > [C₄mim][PF₆] > [C₄mim][BF₄]. So depending on the IL used, the amount of IL within the core of microemulsions can be easily manipulated to directly affect the size of aggregates in microemulsions. The size increase with increasing R value (R value is defined as the molar ratio of RTILs to [C₄mim][AOT]) was found to be maximum in the case of [C₂mim][TF₂N]/[C₄mim][AOT]/benzene microemulsions and follows the trend [C₂mim][TF₂N] > [C₄mim][TF₂N] > [C₆mim][TF₂N]. However, the size increase was almost the same with increase in R value in the case of ILs with different anions. The most promising fact about IL-in-oil microemulsions is their high thermal stability compared to that of aqueous microemulsions, so we investigated the effect of temperature on size of aggregates in microemulsions at R = 1.0. It is evident from dynamic light scattering measurements that the aggregates in microemulsions remain monodisperse in nature with increasing temperature, and in all the cases, the size of aggregates in microemulsions decreases with increasing temperature. The effect of water addition on IL-in-oil (IL/O) microemulsions was also studied in detail. By far, this is the first report where the effect of water addition on microemulsions containing hydrophobic ILs is being reported and compared with microemulsions containing hydrophilic ILs. We observed that the added water has a prominent effect on the microstructure of the microemulsions. In all the cases, ¹H NMR spectra provide more detailed information about intra/intermolecular interactions thus affording a clear picture of locations of (i) the RTILs in RTILs/[C₄mim][AOT]/benzene microemulsions and (ii) the added water molecules in microemulsions.



1. INTRODUCTION

Microemulsions are thermodynamically stable, isotropic transparent mixtures of two immiscible liquids (polar and nonpolar) and an amphiphilic component (usually surfactants and cosurfactants). The microheterogeneous environments present in reverse micelles (RM) and microemulsions hold tremendous promise for applications in different fields owing to the nonstandard environments they present. Often these systems exhibit entirely different chemistry than that observed in homogeneous liquid solutions.^{1,2} Microemulsions are capable of solubilizing both polar as well as nonpolar substances and have wide applications^{3,4} in various fields such as chemical

reactions,⁵ preparation of nanomaterials,⁶ and drug delivery systems.⁷

Most studies focus on microemulsions that utilize water as the polar component in combination with the standard anionic surfactant NaAOT (sodium 1,4-bis(2-ethylhexyl) sulfosuccinate; in this article, we used NaAOT for sodium 1,4-bis(2-ethylhexyl) sulfosuccinate, and for 1,4-bis(2-ethylhexyl) sulfosuccinate anion, we used AOT⁻). These studies place

Received: October 26, 2012

Revised: January 11, 2013

Published: January 11, 2013

side by side the water properties such as polarity, viscosity, conductivity, and hydrogen bonding for bulk water and water confined to reverse micelles.^{8–23} However, in recent years, several reports on nonaqueous microemulsions have appeared in the literature.^{24–30} The focus has now shifted on room temperature ionic liquids (RTILs) since they play important roles in water-in-oil (w/o) microemulsions.^{31–40} RTILs are low melting organic salts that are often associated with green chemistry because they possess certain advantageous properties typically linked to environment friendly solvents, like negligible vapor pressure, wide electrochemical window, nonflammability, high thermal stability, and wide liquid range.³⁴ Because the properties of the RTILs are very much dependent on constituent ions, various RTILs can be designed by prudent combination of cationic and anionic constituents to obtain desired properties and applications. Lü et al.³¹ investigated the critical behavior of water/1-butyl-3-methylimidazolium tetrafluoroborate $[C_4\text{mim}][\text{BF}_4]$ /NaAOT/decane microemulsions with various concentrations of $[C_4\text{mim}][\text{BF}_4]$ and found that the critical temperature decreases significantly with the addition of $[C_4\text{mim}][\text{BF}_4]$. Liu et al.³² employed ionic liquid (IL), $[C_4\text{mim}][\text{BF}_4]$, in place of inorganic salts normally used in microemulsion formulation and showed that the concentration of $[C_4\text{mim}][\text{BF}_4]$ can act as an effective interfacial control parameter for tuning formation of microemulsions. Their study showed that the amount of IL needed for curvature adjustment in ionic microemulsions was less than the amount of NaCl normally used.³² On investigating the influence of the IL 1-ethyl-3-methylimidazolium hexylsulfate, $[C_2\text{mim}][C_6\text{SO}_4]$, on spontaneous formation of microemulsions with ionic surfactants, Rojas et al.³³ found a significant increase of transparent phase region on the addition of the IL. Using three different ILs ($[C_2\text{mim}][\text{Cl}]$, $[C_4\text{mim}][\text{Cl}]$, and $[C_8\text{mim}][\text{Cl}]$), Wei et al.³⁵ showed that the water solubilization capacity of NaAOT in isoctane microemulsions is enhanced at low IL concentrations but decreases at high concentrations of IL. These ILs have the same anionic component, while the cationic component differs in alkyl chain length only. They further showed that the water solubilization capacity increases with an increase in chain length of ILs at low IL concentrations.³⁵ In a more recent study, Wei et al.³⁶ studied the influence of ionic liquid on temperature induced percolation of water/NaAOT/isoctane microemulsions. They showed (i) an increase in percolation temperature (T_p) with the addition of ILs and (ii) an increase in percolation temperature with an increase in alkyl chain length of the imidazolium cation. Moreover, they also showed that the anion of the ILs have little effect on T_p of microemulsions.

While the studies mentioned above involve water as one of the components, water-free IL-based microemulsions are also studied by many groups.^{41–54} In the first report on the formation of IL-in-oil microemulsions, Gao et al.⁴¹ prepared $[C_4\text{mim}][\text{BF}_4]$ /TX-100/cyclohexane microemulsions and characterized them by phase behavior, conductivity measurement, dynamic light scattering measurement, freeze-fracturing electron microscopy, and UV-vis technique. Eastoe et al.⁴² further investigated size and shape of the same microemulsions by small-angle neutron scattering (SANS) measurement. They observed regular swelling behavior of microemulsions with the addition of the IL, which indicates that the volume of dispersed nanodomains is proportional to the amount of IL added.⁴² This study was followed by several other reports on similar systems. In these investigations $[C_4\text{mim}][\text{BF}_4]$, TX-100 and toluene,⁴³ p-xylene,⁴⁴ or benzene⁴⁶ were used as the polar phase,

surfactant, and oil phase, respectively. Li et al.⁴⁵ observed from micropolarity studies that the polarity of IL-in-oil microemulsions increased until the formation of the IL pools, beyond which it remained constant. Moniruzzaman et al.^{55,56} investigated novel ionic liquid-in-oil (IL/O) microemulsions capable of dissolving pharmaceuticals that are insoluble or sparingly soluble in water and most pharmaceutical grade organic liquids.⁵⁵ They showed transdermal drug delivery of acyclovir through IL-assisted microemulsion.⁵⁶

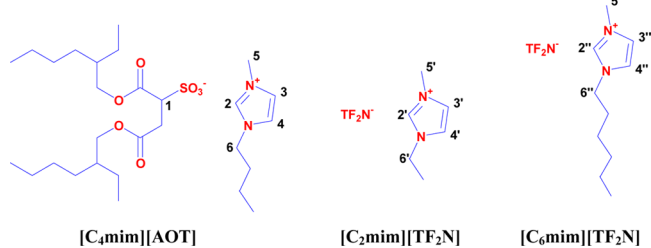
The water-free IL-based microemulsions with charged surfactants are rather scarce.^{47,57–64} Falcone et al. used cationic surfactant, benzyl-*n*-hexadecyldimethylammonium chloride (BHDC) for the formulations of $[C_4\text{mim}][\text{BF}_4]$ /BHDC/benzene and $[C_4\text{mim}][\text{TF}_2\text{N}]$ /BHDC/benzene microemulsions and compared their behavior with $[C_4\text{mim}][\text{BF}_4]$ /TX-100/benzene and $[C_4\text{mim}][\text{TF}_2\text{N}]$ /TX-100/benzene microemulsions.⁴⁷ With their recent multinuclear NMR study on the behavior of $[C_4\text{mim}][\text{BF}_4]$ in $[C_4\text{mim}][\text{BF}_4]$ /BHDC/benzene and $[C_4\text{mim}][\text{BF}_4]$ /TX-100/benzene microemulsions,⁵⁷ they concluded that the structure and behavior of entrapped ILs in the microemulsions depend strongly on the surfactants used.^{47,57} We studied the solvation dynamics of coumarin dyes in $[C_4\text{mim}][\text{BF}_4]$ /BHDC/benzene⁵⁸ and $[\text{Py}][\text{TF}_2\text{N}]$ /BHDC/benzene microemulsions.⁵⁹ After observing surfactant-like behavior of surface active ionic liquid (SAIL) 1-hexadecyl-3-methylimidazolium chloride, $[C_{16}\text{mim}][\text{Cl}]$ in EAN, Zech et al. studied microemulsions RTIL($[C_4\text{mim}][\text{BF}_4]$ and EAN)/ $[C_{16}\text{mim}][\text{Cl}]$ /dodecane using conductivity, DLS, and SAXS measurements.⁶⁰ They concluded that, for preparation of microemulsions with high temperature stability and temperature insensitivity, it is better to use ionic surfactants in combination with ILs.⁶¹ They explored thermal stability of EAN/ $[C_{16}\text{mim}][\text{Cl}]$ /dodecane microemulsions at ambient pressure, which exhibited stability over the temperature range 30 to 150 °C.⁶¹ ILs bearing long alkyl chains with amphiphilic character are named surface active ionic liquids. SAILs possess combined properties of ILs and surfactants.^{62,63,65} Using anionic surfactant NaAOT, Cheng et al.⁶⁶ formulated IL-in-IL microemulsions where they succeeded in dispersing hydrophobic IL, 1-butyl-3-methylimidazolium hexafluorophosphate, $[C_4\text{mim}][\text{PF}_6]$, in hydrophilic IL, propylammonium formate, PAF. Rabe and Koetz⁶⁷ investigated microemulsion formation process in CTAB/IL/toluene/pentanol mixtures. They employed 1-ethyl-3-methylimidazolium ethylsulfate, $[C_2\text{mim}][C_2\text{SO}_4]$, and 1-ethyl-3-methylimidazolium hexylsulfate, $[C_2\text{mim}][C_6\text{SO}_4]$, ILs for microemulsion characterizations. They showed changes in droplet size and droplet-droplet interactions by increasing the amount of IL in the reverse IL-in-oil microemulsions.

In our earlier articles,^{68,69} for the first time we designed a new strategy for creating huge number of IL-in-oil microemulsions with charged surfactants. We showed that by replacing the inorganic cation, Na^+ of NaAOT, with an organic cation and using different ionic liquid as polar core, we can formulate a huge number of microemulsions. Here, we would like to explore (i) the effect of the addition of three different ionic liquids (ILs), 1-ethyl-3-methylimidazolium bis(trifluoromethanesulfonyl)imide $[C_2\text{mim}][\text{TF}_2\text{N}]$, 1-butyl-3-methylimidazolium bis(trifluoromethanesulfonyl)imide $[C_4\text{mim}][\text{TF}_2\text{N}]$, and 1-hexyl-3-methylimidazolium bis(trifluoromethanesulfonyl)imide $[C_6\text{mim}][\text{TF}_2\text{N}]$, on the properties of IL/ $[C_4\text{mim}][\text{AOT}]$ /benzene microemulsions (anionic part of the three ILs is identical, and cationic part

differs in the alkyl chain length only), and (ii) the effect of the addition of $[C_4\text{mim}][\text{TF}_2\text{N}]$, $[C_4\text{mim}][\text{PF}_6]$, and $[C_4\text{mim}][\text{BF}_4]$ ILs on the properties of IL/ $[C_4\text{mim}][\text{AOT}]$ /benzene microemulsions (here cationic part of the three ILs is identical, the anionic parts are different, and the ionic liquids follow $[C_4\text{mim}][\text{TF}_2\text{N}] > [C_4\text{mim}][\text{PF}_6] > [C_4\text{mim}][\text{BF}_4]$ hydrophobicity trend).⁷⁰ We have chosen TF_2N^- containing ionic liquids because they are stable toward hydrolysis⁷¹ and good absorber of carbon dioxide (CO_2).^{72–75} In addition to this, many groups are involved in the investigation of their physicochemical properties.^{76–80} We have also compared the effect of temperature variation on the properties of the microemulsions containing different ionic liquids.

In summary, for the first time, we have shown the formation and characterization of different IL-in-oil microemulsions containing anionic surface active ionic liquid, $[C_4\text{mim}][\text{AOT}]$ as a surfactant molecule, where a comparative study of the effect of ionic liquid having different alkyl chains has been carried out (Scheme 1). In addition to this, we have shown the effect of water addition on microemulsions containing hydrophobic ILs, which is by far the first report of this kind.

Scheme 1. Chemical Structure and Atom Numbering of $[C_4\text{mim}][\text{AOT}]$, $[C_2\text{mim}][\text{TF}_2\text{N}]$, and $[C_6\text{mim}][\text{TF}_2\text{N}]$



2. EXPERIMENTAL SECTION

2.1. Materials and Instrumentation. NaAOT (sodium 1,4-bis(2-ethylhexyl) sulfosuccinate, Sigma-Aldrich) was dried at room temperature in vacuum for 30 h before use. $[C_4\text{mim}][\text{AOT}]$ (synthesized as reported earlier⁶⁸) was dried in vacuum for 50 h at 60–70 °C before use. RTILs $[C_2\text{mim}][\text{TF}_2\text{N}]$, $[C_4\text{mim}][\text{TF}_2\text{N}]$, $[C_6\text{mim}][\text{TF}_2\text{N}]$, and $[C_4\text{mim}][\text{PF}_6]$ were obtained from Merck (high purity grade). RTIL $[C_4\text{mim}][\text{BF}_4]$ was obtained from Kanto chemicals (98% purity). All the RTILs were dried in vacuum for 24 h at ~60 °C before use. Benzene (Spectrochem, HPLC grade) was used as received. Doubly distilled deionized water (Milli-Q water) was used for sample preparation.

For measurement of size and size distribution of aggregates in microemulsions, dynamics light scattering (DLS) measurements were performed with a Malvern Nano ZS instrument employing a 4 mW He–Ne laser ($\lambda = 632.8$ nm). During the process of data collection, scattering photons were collected at a scattering angle of 173°. The scattering intensity data were processed using instrumental software to obtain hydrodynamic diameter (d_h) and size distribution of each sample. The instrument measures fluctuation in scattering intensity and uses this to calculate the size of particles within the sample. The d_h values of microemulsions were estimated from intensity autocorrelation function of time-dependent fluctuation in intensity. The d_h is defined as follows

$$d_h = \frac{k_B T}{3\pi\eta D} \quad (1)$$

where, k_B is the Boltzmann constant, η is viscosity, and D is translational diffusion coefficient.

For viscosity measurements, we used a Brookfield DV-II+ Pro (viscometer). The temperature was maintained by circulating water through the cell holder using a JEIO TECH Thermostat (RW-052GS).

All NMR measurements were carried out with a Bruker 200 MHz NMR spectrometer using $C_6\text{D}_6$ (Aldrich, 99.6 atom % D) as the chemical shift reference for mode locking. Proton-NMR measurements of neat ionic liquids were performed using D_2O as external chemical shift reference. To remove any perturbation to the studied system arising from the presence of D_2O , D_2O was packed in a capillary and then added to NMR tube.

3. RESULTS AND DISCUSSION

3.1. Phase Behavior Study. For characterization of different microemulsions, we performed phase behavior study. We characterized a partial phase diagram of the ternary systems RTILs/ $[C_4\text{mim}][\text{AOT}]$ /benzene at 298 K by observing transition from clear transparent solution to turbid solution visually, i.e., through naked eye (phase boundaries data of all the RTILs/ $[C_4\text{mim}][\text{AOT}]$ /benzene ternary systems are given in Table S1 of the Supporting Information).

3.1.1. Influence of Alkyl Side-Chain Length of Imidazolium Cation. Figure 1 shows phase diagrams of RTILs/ $[C_4\text{mim}][\text{AOT}]$ /benzene ternary systems at 298 K, where RTILs are $[C_2\text{mim}][\text{TF}_2\text{N}]$, $[C_4\text{mim}][\text{TF}_2\text{N}]$, and $[C_6\text{mim}][\text{TF}_2\text{N}]$. We observed that a continuous stable single phase microemulsion region can always be observed over different RTILs or benzene content range of 0–100 wt %. Interestingly, the area of single phase region was found to be maximum in the case of $[C_6\text{mim}][\text{TF}_2\text{N}]$ / $[C_4\text{mim}][\text{AOT}]$ /benzene microemulsions and follows the trend $[C_6\text{mim}][\text{TF}_2\text{N}] > [C_4\text{mim}][\text{TF}_2\text{N}] > [C_2\text{mim}][\text{TF}_2\text{N}]$. Here, it is concluded that the area of the single phase region increases with an increase in the alkyl chain length of cations of the RTILs.

Rabe and Koetz⁶⁷ investigated the influence of cosurfactant and type of IL anion on microemulsion formation process in CTAB/IL/toluene/pentanol mixtures. They employed 1-ethyl-3-methylimidazolium ethylsulfate, $[C_2\text{mim}][\text{C}_2\text{SO}_4]$, and 1-ethyl-3-methylimidazolium hexylsulfate, $[C_2\text{mim}][\text{C}_6\text{SO}_4]$, ILs for characterization of these microemulsions. They showed that, when toluene is partially substituted by pentanol in the case of CTAB/ $[C_2\text{mim}][\text{C}_2\text{SO}_4]$ /toluene/pentanol, the area of single phase region increases, which has been accounted for by the stabilizing effect on interfacial layer. However, for CTAB/ $[C_6\text{mim}][\text{C}_2\text{SO}_4]$ /toluene/pentanol system, a drastic increase in the single phase region was observed.⁶⁷ The difference in the behavior of ILs with an increase in alkyl chain length supports our findings.

The observed difference in the properties of three RTILs arises due to the surface active properties of the IL cations because, in our case, the SAIL is negatively charged. The cations of all the ionic liquids interact with an anionic headgroup of SAIL due to attractive cation–anion interaction. The difference in strength of interaction arises due to the presence of hexyl chain on 1-hexyl-3-methylimidazolium cation, which is responsible for more pronounced penetration because it aids in aligning the cation with the tail part of the AOT[–]

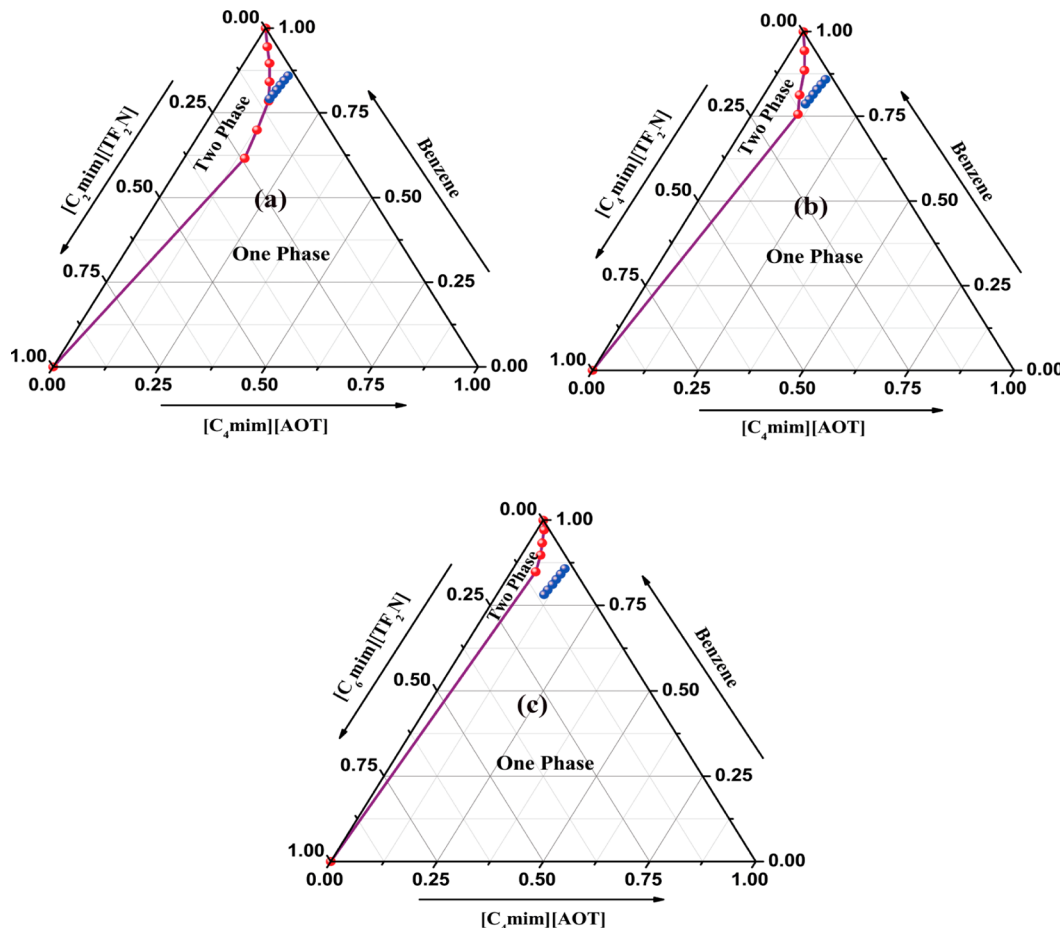


Figure 1. Phase diagrams of the RTILs/[C₄mim][AOT]/benzene ternary systems at 298 K, where RTILs are (a) [C₂mim][TF₂N], (b) [C₄mim][TF₂N], and (c) [C₆mim][TF₂N] (blue points indicate different *R* values selected for the corresponding system).

anion. However, in the case of 1-ethyl-3-methylimidazolium cation, ethyl chain is apparently unsuccessful in functioning similarly due to the inability of 1-ethyl-3-methylimidazolium cation to align itself with the tail part of the AOT⁻ anion. The difference in the strength of interaction between AOT⁻ anion with [C₂mim]⁺ and with [C₆mim]⁺ cations is well supported by ¹H NMR spectra (vide infra). The pronounced penetration and alignment of the cation with the tail part of the AOT⁻ anion makes the interfacial layer more rigid; therefore, the RTIL solubilization capacity increases, and the area of single phase region increases. This increase in rigidity of the interfacial layer with the addition of ILs having long alkyl chain is well supported by Rabe and Koetz⁶⁷ and Wei et al.³⁶ (vide supra).

3.1.2. Influence of RTIL Anion. Figure 2 shows the phase diagrams of RTILs/[C₄mim][AOT]/benzene ternary systems at 298 K, where RTILs are [C₄mim][TF₂N], [C₄mim][PF₆], and [C₄mim][BF₄]. Here, again we observed a continuous stable single phase microemulsion region over different RTILs or benzene content in the range of 0–100 wt %. The area of single phase region was found to be maximum in the case of [C₄mim][TF₂N]/[C₄mim][AOT]/benzene microemulsions and follows the trend [C₄mim][TF₂N] > [C₄mim][PF₆] > [C₄mim][BF₄]. Although we observed some difference in the area of single phase region, the difference is less pronounced compared to that of ionic liquid having different cations. This is due to the absence of attractive interaction between the anion of the RTILs and the negatively charged surfaces of SAIL used for the construction of IL-in-oil microemulsions.

The observed difference in the area of single phase region arises due to different cation–anion interaction strengths of the three ionic liquids.³⁶ Among the three RTILs [C₄mim][TF₂N], [C₄mim][PF₆], and [C₄mim][BF₄], the TF₂N⁻ is the least and BF₄⁻ is the most interacting anion with C₄mim⁺ cation, and they follow BF₄⁻ > PF₆⁻ > TF₂N⁻ order.⁸¹ TF₂N⁻ being the least interacting anion with C₄mim⁺ cation causes strong interaction of C₄mim⁺ with AOT⁻ anion, which makes the interfacial layer more rigid and allows more RTIL to dissolve inside the polar core of the microemulsions (causes an increase in the single phase region).

3.2. Size of the Aggregates in Microemulsions: Dynamic Light Scattering Measurements. Although the phase behavior study indicates formation of microemulsions of RTILs/[C₄mim][AOT]/benzene ternary systems, the important question that we need to answer is whether the ionic liquid is entrapped effectively by the surfactant molecules creating IL-in-oil microemulsions. To answer this question, we used a dynamic light scattering (DLS) measurement since it is a powerful technique, widely used to assess whether the ILs are encapsulated by the surfactant molecules to create microemulsion media.^{58,82} For all the measurements, we have used 0.2 M [C₄mim][AOT] in benzene solution. Extensive studies on the characterization of microemulsions using DLS show that, if the IL is really encapsulated to form IL-in-oil microemulsions, the size of the droplets must increase regularly as the *R* value (here the *R* value is defined as the molar ratio of RTILs to [C₄mim][AOT]) to a certain level.^{47,54,58,82,83} The

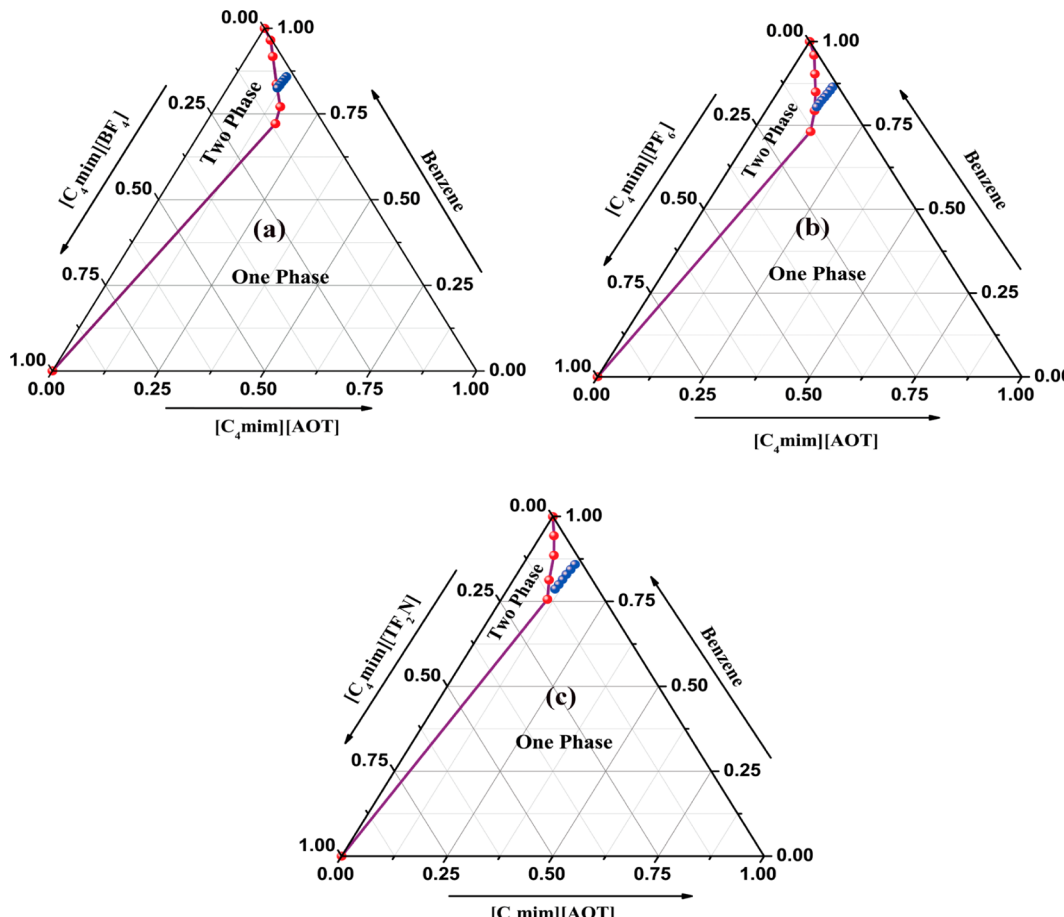


Figure 2. Phase diagrams of the RTILs/[C₄mim][AOT]/benzene ternary systems at 298 K, where RTILs are (a) [C₄mim][BF₄], (b) [C₄mim][PF₆], and (c) [C₄mim][TF₂N] (blue points indicate different R values selected for the corresponding system).

observed swelling behavior is consistent with the volume of dispersed nanodomains being directly proportional to the amount of added ILs. This type of behavior is common to many well established NaAOT stabilized w/o microemulsions. The microemulsion media consists of discrete spherical and noninteracting droplets of ILs stabilized by the surfactant showing regular increase in the size of the droplets (linearly with increasing R value).⁴⁷ Deviations from linearity could be observed due to many reasons, the most relevant ones being droplet–droplet interaction and shape of the microemulsions.⁴⁷

3.2.1. Influence of Alkyl Side-Chain Length of Imidazolium Cation. Figure 3 shows the size distributions and variation of size of RTILs/[C₄mim][AOT]/benzene ternary systems with increasing R values at 298 K, where RTILs are [C₂mim][TF₂N], [C₄mim][TF₂N], and [C₆mim][TF₂N]. In all the cases, DLS studies revealed the formation of the IL-in-oil microemulsion. The sizes of the aggregates increased from 5.1, 5.4, and 5.0 nm to 44.2, 17.7, and 9.4 nm with increasing R values from 0.2 to 1.2 for [C₂mim][TF₂N], [C₄mim][TF₂N], and [C₆mim][TF₂N], respectively (Table 1). We observed almost linear variations of size at R values lower than 1.0, 1.2, and 1.6 in the case of [C₂mim][TF₂N], [C₄mim][TF₂N], and [C₆mim][TF₂N], respectively (Figure 3b (inset)). We observed deviation from linearity at R values higher than 1.0 and 1.2 in the case of [C₂mim][TF₂N] and [C₄mim][TF₂N], respectively, which may be attributed to the increased droplet–droplet interaction at higher R value.⁴⁷ Interestingly, we did not observe any deviation from the linearity in size variation of

[C₆mim][TF₂N]/[C₄mim][AOT]/benzene aggregates in microemulsions, which again indicates that the microemulsion media consist of discrete spherical and noninteracting droplets. The difference in the behavior of three ionic liquids can be rationalized by considering the underlying stabilizing interactions that enable the formation of IL-in-oil microemulsions. We mentioned above that the presence of hexyl chain on 1-hexyl-3-methylimidazolium cation causes more pronounced penetration compared to 1-ethyl-3-methylimidazolium cation because hexyl chain aids in aligning the cation with the tail part of AOT⁻ anion (vide supra). The pronounced penetration and alignment of the cation with the tail part of AOT⁻ anion reduces the effective headgroup area of the surfactant by screening electrostatic repulsions. This causes increase in the curvature parameter of the surfactant, making the interfacial layer more rigid in the case of [C₆mim][TF₂N]/[C₄mim][AOT]/benzene microemulsions, decreasing attractive interactions between droplets and consequently preventing coalescence of droplets. This is also well supported by observation of Wei et al.³⁵

Another noteworthy observation is that the increase in the size of aggregate is maximum for [C₂mim][TF₂N]/[C₄mim][AOT]/benzene microemulsions and that it follows the trend [C₂mim][TF₂N] > [C₄mim][TF₂N] > [C₆mim][TF₂N] (Table 1). These variations arise due to the change of the curvature parameter of SAIL (vide supra). Liu et al.⁸⁴ showed that the droplet size of aggregates in microemulsions can directly bring out the effect of additives on the curvature

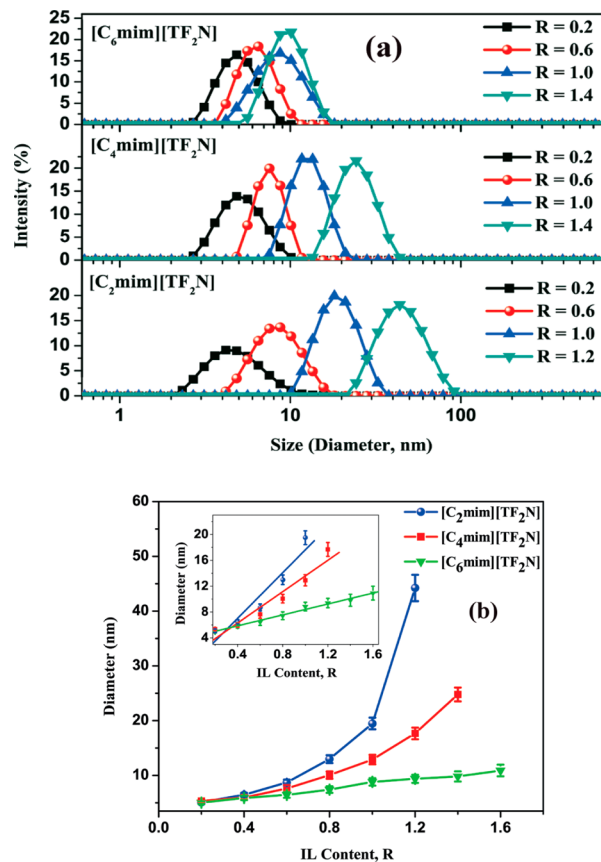


Figure 3. (a) Size distribution of the droplets (measured by dynamic light scattering) of RTILs/[C₄mim][AOT]/benzene microemulsions at different *R* values. (b) Diameter of the droplets of RTILs/[C₄mim][AOT]/benzene microemulsion as a function of RTIL concentration (*R* value). The RTILs are [C₂mim][TF₂N], [C₄mim][TF₂N], and [C₆mim][TF₂N].

parameter of surfactant. The increase in the droplet size of aggregates in microemulsions corresponds to a decrease in the curvature parameter of surfactant.

3.2.2. Influence of RTIL Anion. Figure 4 shows the size distributions and variation of size of RTILs/[C₄mim][AOT]/benzene ternary systems with increasing *R* values at 298 K, where RTILs are [C₄mim][TF₂N], [C₄mim][PF₆], and [C₄mim][BF₄]. Here, also the DLS studies revealed the formation of the IL-in-oil microemulsion. The sizes of the aggregates increased from 5.4, 4.9, and 4.3 nm to 17.7, 21.0, and 18.7 nm with increasing *R* values from 0.2 to 1.2 in the case of [C₄mim][TF₂N], [C₄mim][PF₆], and [C₄mim][BF₄], respectively (Table 1). We observed almost linear variations of size at *R* values lower than 1.0 in all the cases (Figure 4b (inset)). Unlike ILs where cations of ILs differ in alkyl chain length, here, the size increase is almost the same with an increase in *R* value. This difference arises due to the absence of attractive interaction between anion of the RTILs and the negatively charged surfaces of SAIL used for the construction of IL-in-oil microemulsions (vide supra).

3.2.3. Influence of Temperature on the Size of the Aggregates in Microemulsions. We investigated the effect of temperature on the size of the aggregates in RTILs/[C₄mim][AOT]/benzene microemulsions at *R* = 1.0 (Figures 5 and 6). It is evident from the dynamic light scattering measurements that the microemulsions are monodisperse in

Table 1. Size (Diameter) of the Droplets of RTILs/[C₄mim][AOT]/Benzene Microemulsions As a Function of Concentration of RTILs (*R* Value) at 298 K

system	<i>R</i> value	size (diameter, nm)
[C ₂ mim][TF ₂ N]/[C ₄ mim][AOT]/benzene	0.2	5.1 ± 0.3
	0.4	6.5 ± 0.3
	0.6	8.7 ± 0.5
	0.8	13.0 ± 0.7
	1.0	19.5 ± 1.1
	1.2	44.2 ± 2.4
	0.2	5.4 ± 0.2
	0.4	6.0 ± 0.2
	0.6	7.6 ± 0.6
	0.8	10.1 ± 0.7
[C ₄ mim][TF ₂ N]/[C ₄ mim][AOT]/benzene	1.0	12.9 ± 0.9
	1.2	17.7 ± 1.1
	1.4	24.8 ± 1.3
	0.2	5.0 ± 0.3
	0.4	5.9 ± 0.4
	0.6	6.5 ± 0.5
	0.8	7.4 ± 0.6
	1.0	8.8 ± 0.7
	1.2	9.4 ± 0.7
	1.4	9.8 ± 0.9
[C ₄ mim][PF ₆]/[C ₄ mim][AOT]/benzene	1.6	10.9 ± 1.1
	0.2	4.9 ± 0.2
	0.4	5.8 ± 0.3
	0.6	7.1 ± 0.4
	0.8	9.1 ± 0.5
	1.0	12.9 ± 0.6
	1.2	21.0 ± 1.1
	1.4	64.6 ± 3.2
[C ₄ mim][BF ₄]/[C ₄ mim][AOT]/benzene	0.2	4.3 ± 0.2
	0.4	5.2 ± 0.3
	0.6	6.9 ± 0.3
	0.8	8.9 ± 0.4
	1.0	12.3 ± 0.6
	1.2	18.7 ± 0.9

nature, and in all the cases, the size of aggregates in microemulsions decreases with increasing temperature. The observed decrease in size with increase in temperature indicates the noninteracting hard sphere nature of the aggregates in RTILs/[C₄mim][AOT]/benzene microemulsions at *R* = 1.0 and absence of any droplet coalescing process.^{47,69,85} In other words, the microemulsions retain their structural integrity across the temperature range used in the study. The decrease in size with increase in temperature is well supported by our earlier reports,^{54,69} where we showed that the size of the [C₄mim][BF₄]/BHDC/benzene and [Py][TF₂N]/[C₄mim][AOT]/benzene aggregates in microemulsions decreases with an increase in temperature.^{54,69}

Interestingly, the sizes of the aggregates at *R* = 1.0 decreased from 25.2, 14.5, and 10.0 nm to 8.8, 7.2, and 6.1 nm with increasing temperature from 293 to 328 K in the case of [C₂mim][TF₂N], [C₄mim][TF₂N], and [C₆mim][TF₂N], respectively (Table 2). We observed almost linear variations of size with temperature. Figure 5b clearly indicates that the slope of the linear fit is maximum in the case of [C₂mim][TF₂N] and follows the trend [C₂mim][TF₂N] > [C₄mim][TF₂N] > [C₆mim][TF₂N]. The observed difference in the behavior of three microemulsions arises due to the difference in

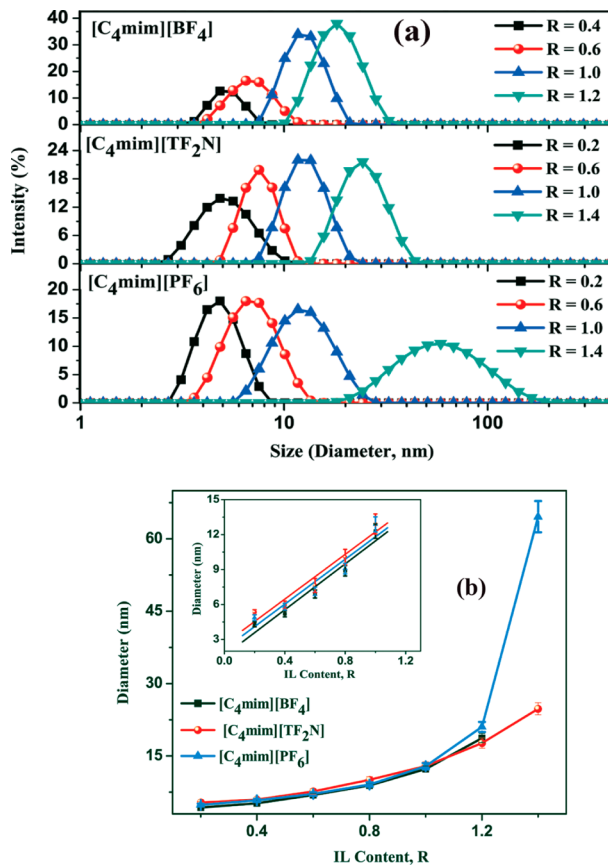


Figure 4. (a) Size distribution of the droplets (measured by dynamic light scattering) of RTILs/[C₄mim][AOT]/benzene microemulsions at different R values. (b) Diameter of the droplets of RTILs/[C₄mim][AOT]/benzene microemulsion as a function of RTILs concentration (R value). The RTILs are [C₄mim][BF₄], [C₄mim][PF₆], and [C₄mim][TF₂N].

the rigidity of the microemulsions. The [C₆mim][TF₂N]/[C₄mim][AOT]/benzene microemulsion being more rigid in nature (vide supra) shows less temperature dependence compared to the [C₂mim][TF₂N]/[C₄mim][AOT]/benzene microemulsion.

However the sizes of the aggregates at $R = 1.0$ decreased from 14.5, 14.2, and 13.6 nm to 7.4, 9.2, and 8.9 nm with increasing temperature from 293 to 323 K in the case of [C₄mim][TF₂N], [C₄mim][PF₆], and [C₄mim][BF₄], respectively (Table 2). Here, also we observed almost linear variations of size with temperature, but the slope of linear fit almost remains the same (Figure 6b). So the observed uniform decrease in size in the case of the three microemulsions arises due to almost the same rigidity of microemulsions.

3.2.4. Influence of Water Addition on the Size of the Aggregates in Microemulsions. **3.2.4.1. Influence of Alkyl Side-Chain Length of Imidazolium Cation.** We investigated the effect of water addition on the size of aggregates in RTILs/[C₄mim][AOT]/benzene microemulsions at $R = 1.0$ (at 298 K). Here, also we used 0.2 M [C₄mim][AOT] in benzene solution for all the measurements. Considering the extremely limited solubility of [C₂mim][TF₂N], [C₄mim][TF₂N], and [C₆mim][TF₂N],⁷⁰ it is interesting to investigate the effect of water addition on the behavior of microemulsions. Here, it is evident from dynamic light scattering measurements that the microemulsions are monodisperse in nature, and in all the

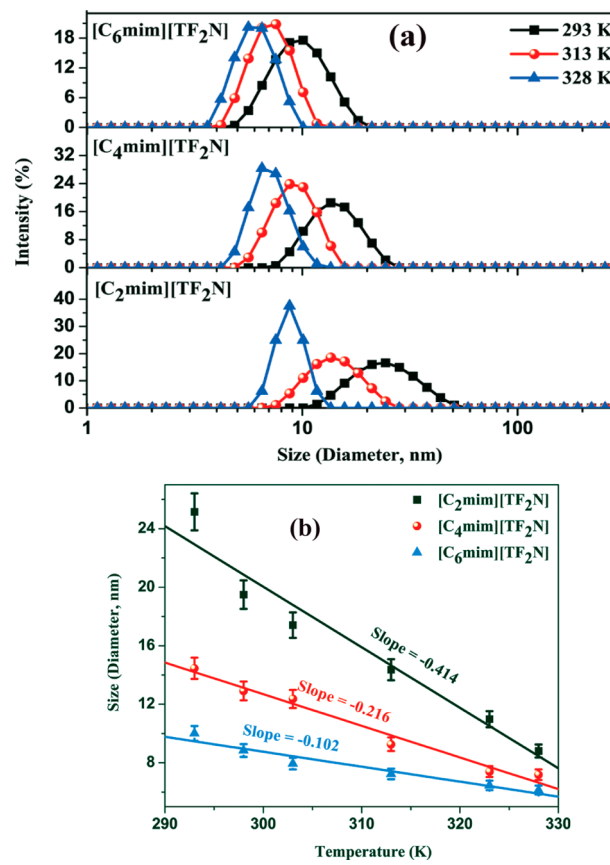


Figure 5. (a) Size distribution of the droplets (measured by dynamic light scattering) of RTILs/[C₆mim][AOT]/benzene microemulsions ($R = 1.0$) at different temperatures. (b) Diameter of the droplets of RTILs/[C₆mim][AOT]/benzene microemulsion ($R = 1.0$) as a function of temperature. The RTILs are [C₂mim][TF₂N], [C₄mim][TF₂N], and [C₆mim][TF₂N].

cases, the size of aggregates in microemulsions increases with increasing water content (Figures 7).

Interestingly, the sizes of the aggregates at $R = 1.0$ (at 298 K) increases from 19.5, 12.9, and 8.8 nm to 78.3, 21.4, and 12.5 nm with increasing water content from 0 to 300 mM in the case of [C₂mim][TF₂N], [C₄mim][TF₂N], and [C₆mim][TF₂N], respectively (Table 3). Figure 7b shows the variations of size with increasing water content, which clearly indicates that the size variation is almost linear in the case of [C₄mim][TF₂N] and [C₆mim][TF₂N], whereas slight deviation from linearity is observed in the case of [C₂mim][TF₂N]. The increase in size with the addition of 300 mM water was found to be maximum in the case of [C₂mim][TF₂N]/[C₄mim][AOT]/benzene microemulsions and follows the trend [C₂mim][TF₂N] > [C₄mim][TF₂N] > [C₆mim][TF₂N]. According to Liu et al.,⁸⁴ the decrease in the curvature parameter of the surfactant molecule with the addition of water in [C_nmim][TF₂N]/[C₄mim][AOT]/benzene microemulsions follows the trend [C₂mim][TF₂N] > [C₄mim][TF₂N] > [C₆mim][TF₂N]. So the maximum decrease in curvature parameter was observed in the case of [C₂mim][TF₂N]/[C₄mim][AOT]/benzene microemulsions, which is also supported by ¹H NMR spectra (vide infra). This observed difference can be explained by considering the water insolubility in [C_nmim][TF₂N] ionic liquids. The added water molecule being insoluble in [C_nmim][TF₂N] locates itself in the interfacial region of the microemulsions and

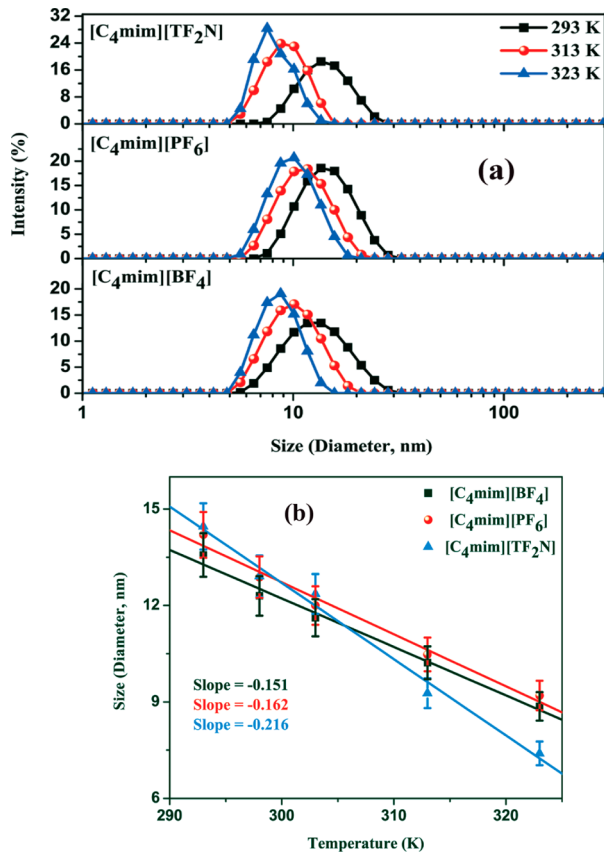


Figure 6. (a) Size distribution of the droplets (measured by dynamic light scattering) of RTILs/[C₄mim][AOT]/benzene microemulsions ($R = 1.0$) at different temperatures. (b) Diameter of the droplets of RTILs/[C₄mim][AOT]/benzene microemulsion ($R = 1.0$) as a function of temperature. The RTILs are [C₄mim][BF₄], [C₄mim][PF₆], and [C₄mim][TF₂N].

replaces some of the [C_nmim]⁺ cation and decreases the curvature of the surfactant. The replacement of cation [C_nmim]⁺ with added water molecules is more efficient in the case of [C₂mim][TF₂N]/[C₄mim][AOT]/benzene microemulsions owing to relatively weak interaction between [C₂mim]⁺ and AOT⁻ compared to [C₆mim]⁺ and AOT⁻, which causes an increase in the effective surface area and decrease in curvature parameter. This observation is well supported by Wei et al.,³⁵ where they showed that the long-chain IL makes the interfacial layer more rigid compared to that of small chain IL (vide supra).

3.2.4.2. Influence of RTIL Anion. It is really interesting to compare the effect of water addition in different microemulsions containing IL of different hydrophobicity, where hydrophobicity follows the trend [C₄mim][TF₂N] > [C₄mim][PF₆] > [C₄mim][BF₄].⁷⁰ The sizes of the aggregates at $R = 1.0$ (at 298 K) increase from 12.9, 12.9, and 12.3 nm to 21.4, 20.3, and 14.6 nm with increasing water content from 0 to 300 mM in the case of [C₄mim][TF₂N], [C₄mim][PF₆], and [C₄mim][BF₄], respectively (Table 3). Figure 8 shows the distributions and variations of size with increasing water content, which clearly indicates that the size variation is almost linear in all the cases. The increase in size with the addition of 300 mM of water was found to be maximum in the case of [C₄mim][TF₂N]/[C₄mim][AOT]/benzene microemulsions and follows the trend [C₄mim][TF₂N] > [C₄mim][PF₆] > [C₄mim][BF₄]. So the increase in size of aggregates in microemulsions with the

Table 2. Size (Diameter) of the Droplets of RTILs/[C₄mim][AOT]/Benzene Microemulsions at $R = 1.0$ As a Function of Temperature

system	temperature (K)	size (diameter, nm)
[C ₂ mim][TF ₂ N]/[C ₄ mim][AOT]/benzene	293	25.2 ± 1.3
	298	19.5 ± 1.1
	303	17.4 ± 0.9
	313	14.4 ± 0.7
	323	11.0 ± 0.5
	328	8.8 ± 0.4
	323	7.4 ± 0.4
[C ₄ mim][TF ₂ N]/[C ₄ mim][AOT]/benzene	293	14.5 ± 0.7
	298	12.9 ± 0.9
	303	12.4 ± 0.6
	313	9.3 ± 0.5
	323	7.2 ± 0.4
	328	7.2 ± 0.4
	323	6.4 ± 0.3
[C ₆ mim][TF ₂ N]/[C ₄ mim][AOT]/benzene	293	10.0 ± 0.5
	298	8.8 ± 0.7
	303	7.9 ± 0.4
	313	7.2 ± 0.4
	323	6.4 ± 0.3
	328	6.1 ± 0.3
	323	5.5 ± 0.3
[C ₄ mim][PF ₆]/[C ₄ mim][AOT]/benzene	293	14.2 ± 0.7
	298	12.9 ± 0.6
	303	12.0 ± 0.6
	313	10.5 ± 0.5
	323	9.2 ± 0.5
	323	8.9 ± 0.4
	323	8.9 ± 0.4
[C ₄ mim][BF ₄]/[C ₄ mim][AOT]/benzene	293	13.6 ± 0.7
	298	12.3 ± 0.6
	303	11.6 ± 0.6
	313	10.2 ± 0.5
	323	9.2 ± 0.5
	323	8.9 ± 0.4
	323	8.9 ± 0.4

addition of water follows exactly the same trend as the hydrophobicity of the IL. The added water molecules being insoluble in [C₄mim][TF₂N]/[C₄mim][PF₆] locate themselves in the interfacial region of the microemulsions and replace some of the [C₄mim]⁺ cation, which causes an increase in the effective surface area and a decrease in curvature parameter. The decrease in curvature parameter is manifested by an increase in size. In contrast to this, the added water molecules are highly soluble in the polar core ([C₄mim][BF₄]) of the [C₄mim][BF₄]/[C₄mim][AOT]/benzene microemulsions. Hence, the surface area or curvature of the surfactant molecules remains unchanged, and the increase in size is minimum. This is also supported by ¹H NMR spectra (data not shown in this article).

3.3. ¹H NMR Spectra. ¹H NMR spectra are taken to provide more detailed information about the intra/intermolecular interactions and thus provide the microstructure characteristics of the IL-in-oil microemulsions including the locations of the RTILs in RTILs/[C₄mim][AOT]/benzene microemulsions. For all the measurements, we used 0.2 M [C₄mim][AOT] in benzene solution. First, we compare the proton signal associated with the imidazolium ring of [C₄mim][AOT] in [C₄mim][AOT]/benzene reverse micelle and in neat [C₂mim][TF₂N] and [C₆mim][AOT] (Figures 9). The H₂ signal in the case of [C₄mim][AOT] appeared at significantly downfield position ($\delta = 9.356$ ppm) compared to that of H_{2'} of [C₂mim][TF₂N] ($\delta = 8.461$ ppm) and H_{2''} of [C₆mim][TF₂N] ($\delta = 8.548$ ppm). In contrast to this, the

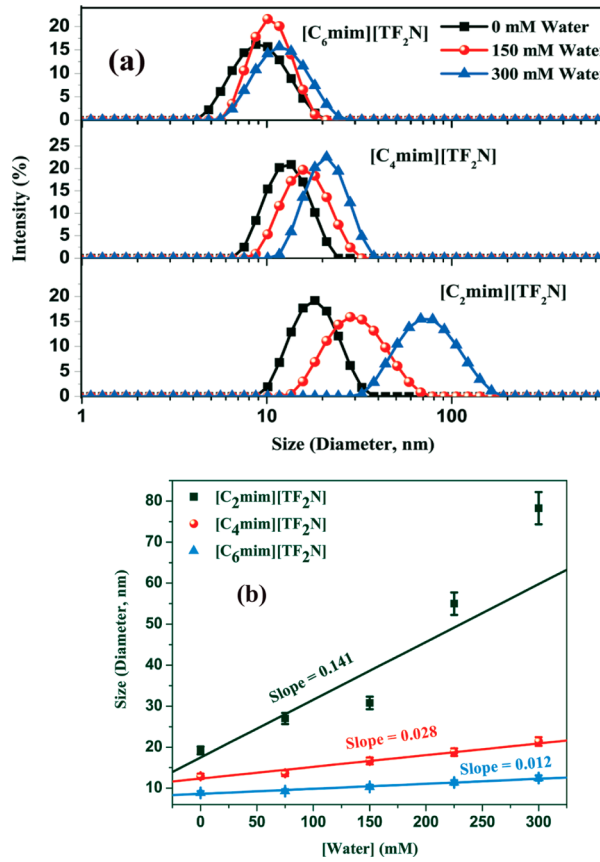


Figure 7. (a) Size distribution of the droplets (measured by dynamic light scattering) of RTILs/ $[C_4\text{mim}][\text{AOT}]$ /benzene microemulsions ($R = 1.0$) with different water content. (b) Diameter of the droplets of RTILs/ $[C_4\text{mim}][\text{AOT}]$ /benzene microemulsion ($R = 1.0$) as a function of water content. The RTILs are $[C_2\text{mim}][\text{TF}_2\text{N}]$, $[C_4\text{mim}][\text{TF}_2\text{N}]$, and $[C_6\text{mim}][\text{TF}_2\text{N}]$.

other two protons of the imidazolium ring also shifted to downfield position, but the shift is relatively small compared to that of H2 protons. This can be accounted for by the acidity of the H2 hydrogen atom, which makes it most sensitive to its environment.^{57,85}

Figures 9 and 10 show a part of the ^1H NMR spectra of neat ILs and RTILs/ $[C_4\text{mim}][\text{AOT}]$ /benzene microemulsions at different R value (full NMR is shown in Figures S1 and S2 of the Supporting Information). With the addition of IL $[C_2\text{mim}][\text{TF}_2\text{N}]$ in $[C_4\text{mim}][\text{AOT}]$ /benzene reverse micelle, the H2' proton of $[C_2\text{mim}][\text{TF}_2\text{N}]$ is significantly shifted downfield compared to the neat $[C_2\text{mim}][\text{TF}_2\text{N}]$ ($\delta = 8.461$ ppm) (Figure 9A). In $[C_2\text{mim}][\text{TF}_2\text{N}]$ / $[C_4\text{mim}][\text{AOT}]$ /benzene microemulsions (at $R = 0.2$), the signal associated with the H2' proton of $[C_2\text{mim}][\text{TF}_2\text{N}]$ appears at $\delta = 9.356$ ppm, which is 0.895 ppm shifted downfield compared to neat $[C_2\text{mim}][\text{TF}_2\text{N}]$. This huge downfield shift is well supported by many other studies and confirms the incorporation of IL inside the reverse micelle.^{57,64} With further addition of IL, $[C_2\text{mim}][\text{TF}_2\text{N}]$, i.e., with increasing R value from 0.2 to 1.0, the peaks associated with the H2' proton of $[C_2\text{mim}][\text{TF}_2\text{N}]$ and H2 proton of $[C_4\text{mim}][\text{AOT}]$ are shifted upfield from 9.150 and 9.239 ppm to 8.754 and 8.858 ppm, respectively (Figure 11a). This observation is also supported by Falcone et al.⁵⁷ and Ferreyra et al.⁶⁴ Even though the H2' protons signal of $[C_2\text{mim}][\text{TF}_2\text{N}]$ in microemulsions shifted upfield toward the

Table 3. Size (Diameter) of the Droplets of RTILs/ $[C_4\text{mim}][\text{AOT}]$ /Benzene Microemulsions at $R = 1.0$ As a Function of Water Content

system	[water] (mM)	size (diameter, nm)
$[C_2\text{mim}][\text{TF}_2\text{N}]$ / $[C_4\text{mim}][\text{AOT}]$ /benzene	0	19.5 ± 1.1
	75	27.0 ± 1.4
	150	30.8 ± 1.5
	225	55.0 ± 2.7
	300	78.3 ± 3.9
$[C_4\text{mim}][\text{TF}_2\text{N}]$ / $[C_4\text{mim}][\text{AOT}]$ /benzene	0	12.9 ± 0.9
	75	13.6 ± 0.7
	150	16.6 ± 0.8
	225	18.8 ± 0.9
	300	21.4 ± 1.1
$[C_6\text{mim}][\text{TF}_2\text{N}]$ / $[C_4\text{mim}][\text{AOT}]$ /benzene	0	8.8 ± 0.7
	75	9.3 ± 0.5
	150	10.3 ± 0.5
	225	11.4 ± 0.6
	300	12.5 ± 0.6
$[C_4\text{mim}][\text{PF}_6]$ / $[C_4\text{mim}][\text{AOT}]$ /benzene	0	12.9 ± 0.6
	75	13.9 ± 0.7
	150	15.3 ± 0.8
	225	17.6 ± 0.9
	300	20.3 ± 1.0
$[C_4\text{mim}][\text{BF}_4]$ / $[C_4\text{mim}][\text{AOT}]$ /benzene	0	12.3 ± 0.6
	75	12.5 ± 0.6
	150	12.9 ± 0.6
	225	14.1 ± 0.7
	300	14.6 ± 0.7

neat IL with increasing R value, it remains substantially different from neat $[C_2\text{mim}][\text{TF}_2\text{N}]$. This once again indicates a new environment for $[C_2\text{mim}][\text{TF}_2\text{N}]$ in $[C_2\text{mim}][\text{TF}_2\text{N}]$ / $[C_4\text{mim}][\text{AOT}]$ /benzene microemulsions. A similar behavior is observed in the case of $[C_4\text{mim}][\text{TF}_2\text{N}]$ and $[C_6\text{mim}][\text{TF}_2\text{N}]$ (Figure 11b,c shows the variation for $[C_6\text{mim}][\text{TF}_2\text{N}]$; variation for $[C_4\text{mim}][\text{TF}_2\text{N}]$ is not shown here).

We also compared our results with that of Falcone et al.⁵⁷ They showed that, with the addition of $[C_4\text{mim}][\text{BF}_4]$ in the cationic BHDC-based microemulsions, the protons on the $[C_4\text{mim}]^+$ butyl and methyl group closer to the acidic proton of the imidazolium ring display larger shifts than the two protons on the opposite side of the imidazolium ring. They interpreted their observation as the directionality in the interaction was sensed by different protons.⁵⁷ In our study, with the addition of $[C_n\text{mim}][\text{TF}_2\text{N}]$ ionic liquids in anionic $[C_4\text{mim}][\text{AOT}]$ -based microemulsions, the protons on the $[C_n\text{mim}]^+$ alkyl and methyl group near H2 (H5 and H6) display smaller shifts than H3 and H4, the two protons on the opposite side of the imidazolium ring. So, here also we observed directionality in the interaction between added ILs and surfactant molecules. The observed directionality is opposite to that observed by Falcone et al.,⁵⁷ which can be accounted for by the different nature of the surfactant molecule (BHDC is a cationic surfactant, and $[C_4\text{mim}][\text{AOT}]$ is an anionic surfactant), leading to difference in the interaction with the $[C_4\text{mim}]^+$.

We also monitored the signals associated with the surfactant, $[C_4\text{mim}][\text{AOT}]$ molecule, because the surfactant's protons were used to probe the microenvironment created in the microemulsions.^{57,64} We observed a modest but observable chemical shift change, in the signals associated with the

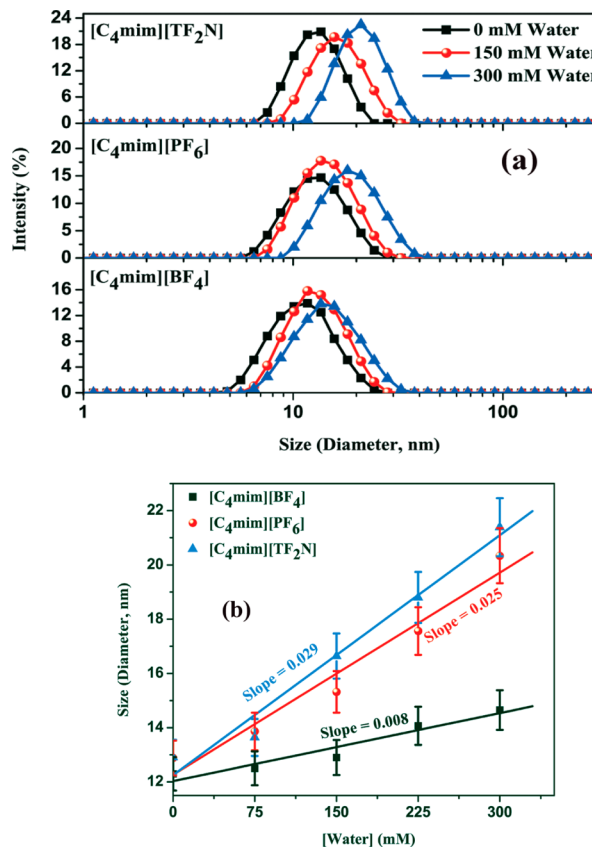


Figure 8. (a) Size distribution of the droplets (measured by dynamic light scattering) of RTILs/ $[C_4\text{mim}][\text{AOT}]$ /benzene microemulsions ($R = 1.0$) with different water content. (b) Diameter of the droplets of RTILs/ $[C_4\text{mim}][\text{AOT}]$ /benzene microemulsion ($R = 1.0$) as a function of water content. The RTILs are $[C_4\text{mim}][\text{BF}_4]$, $[C_4\text{mim}][\text{PF}_6]$, and $[C_4\text{mim}][\text{TF}_2\text{N}]$.

surfactant, $[C_4\text{mim}][\text{AOT}]$ molecule, which demonstrates significant changes in structural organization.^{57,64} Figures 9 and 10 show the variation of ^1H NMR chemical shift of the proton nearest to the polar headgroup of RTIL/ $[C_4\text{mim}][\text{AOT}]$ /benzene microemulsions studied at different R values. The H1 peak of the anion of the $[C_4\text{mim}][\text{AOT}]$, which shows doublet-of-doublet, display upfield shifts as R value increases (in the case of all the ionic liquids studied). This upfield shift of the surfactant molecule with the addition of ILs is well supported by Falcone et al.⁵⁷ and Ferreyra et al.⁶⁴ and suggests the interaction of added ionic liquids with the surfactant molecules. It is noteworthy to mention that, with the addition of ILs, we observed significantly larger shifts for the $[C_4\text{mim}][\text{AOT}]$ surfactant signals arising from protons, closer to the headgroup of $[C_4\text{mim}][\text{AOT}]$ compared to that of the long alkyl chains (negligible change is observed, Figures S1 and S2 of the Supporting Information). These observations once again suggest the incorporation of ILs in the polar core of the microemulsions, where the ILs interact specifically with the headgroup of the surfactant molecules.

We mentioned earlier that the cations of all the ionic liquids interact with the anionic headgroup of the SAIL, $[C_4\text{mim}][\text{AOT}]$, due to the attractive cation–anion interaction, and the difference in the strength of interaction arises due to the presence of different lengths of alky-chains of the added IL cation ($[C_2\text{mim}]^+$, $[C_4\text{mim}]^+$, and $[C_6\text{mim}]^+$). Thus, depending on the strength of the interaction, we expect a difference in

the shift of peak positions. In reality, we observed the same. On going from neat $[C_2\text{mim}][\text{TF}_2\text{N}]$ to $[C_2\text{mim}][\text{TF}_2\text{N}]/[C_4\text{mim}][\text{AOT}]$ /benzene microemulsions at $R = 0.2$, the chemical shift value of HS' proton changes from 3.805 to 3.709 ppm, whereas on going from neat $[C_6\text{mim}][\text{TF}_2\text{N}]$ to $[C_6\text{mim}][\text{TF}_2\text{N}]/[C_4\text{mim}][\text{AOT}]$ /benzene microemulsions at $R = 0.2$, the chemical shift value of HS" proton changes from 3.848 to 3.695 ppm (Figure 10). So, upfield shifts of 0.096 and 0.153 ppm were observed with the incorporation of $[C_2\text{mim}][\text{TF}_2\text{N}]$ and $[C_6\text{mim}][\text{TF}_2\text{N}]$ in microemulsions (Figure 11a,b). The relatively larger change in the case of $[C_6\text{mim}][\text{TF}_2\text{N}]$ incorporation confirms the stronger interaction with the surfactant. A similar behavior is observed when we consider H6' and H6" protons of the $[C_2\text{mim}][\text{TF}_2\text{N}]$ and $[C_6\text{mim}][\text{TF}_2\text{N}]$ ionic liquids (Figure 10).

3.3.1. Effect of Water Addition. Having investigated the effect of water addition on the size of aggregates in microemulsions, we found that the increase in size with the addition of water (final concentration of water was 300 mM) was maximum in the case of $[C_2\text{mim}][\text{TF}_2\text{N}]/[C_4\text{mim}][\text{AOT}]$ /benzene microemulsions (vide supra). Considering that fact, we can say that, with the addition of water, larger perturbation is observed in the case of $[C_2\text{mim}][\text{TF}_2\text{N}]/[C_4\text{mim}][\text{AOT}]$ /benzene microemulsions. Moreover, similar behavior is manifested in the proton-NMR spectra. ^1H NMR spectroscopic analysis was performed because it provides more detailed information about the interaction between the added water molecule with the surfactant and ionic liquid present in the microemulsions and thus provides insight into the solubilization information of added water molecules in the IL-in-oil microemulsions.³⁸ A relatively larger shift in all the NMR peaks were observed with the addition of water to $[C_2\text{mim}][\text{TF}_2\text{N}]/[C_4\text{mim}][\text{AOT}]$ /benzene microemulsions compared to $[C_6\text{mim}][\text{TF}_2\text{N}]/[C_4\text{mim}][\text{AOT}]$ /benzene microemulsions (Figures 9 and 10). With the addition of water (final concentration of water was 300 mM) in the $[C_2\text{mim}][\text{TF}_2\text{N}]/[C_4\text{mim}][\text{AOT}]$ /benzene microemulsions (at $R = 1.0$), the chemical shift value of the HS proton of the surfactant changes from 3.534 to 3.590 ppm, whereas in the case of $[C_6\text{mim}][\text{TF}_2\text{N}]/[C_4\text{mim}][\text{AOT}]$ /benzene microemulsions (at $R = 1.0$), it changes from 3.481 to 3.515 ppm. So, downfield shifts of 0.056 and 0.034 ppm were observed with the addition of 300 mM water to $[C_2\text{mim}][\text{TF}_2\text{N}]$ and $[C_6\text{mim}][\text{TF}_2\text{N}]$ containing microemulsions, respectively (Figures 10). Similar behavior is observed when we consider the HS' and HS" peaks of $[C_2\text{mim}][\text{TF}_2\text{N}]$ and $[C_6\text{mim}][\text{TF}_2\text{N}]$, respectively. Downfield shifts of 0.061 and 0.034 ppm were observed in the HS' and HS" peaks of $[C_2\text{mim}][\text{TF}_2\text{N}]$ and $[C_6\text{mim}][\text{TF}_2\text{N}]$, respectively, with the addition of 300 mM water to the respective microemulsions. In addition to this, the quartet of the H6' proton of $[C_2\text{mim}][\text{TF}_2\text{N}]$ and the triplet of the H6" proton of $[C_6\text{mim}][\text{TF}_2\text{N}]$ are downfield shifted by 0.053 and 0.013 ppm, respectively. So the relatively larger change in the NMR peak position of both surfactant and ionic liquid with the addition of water to $[C_2\text{mim}][\text{TF}_2\text{N}]/[C_4\text{mim}][\text{AOT}]$ /benzene microemulsions compared to the $[C_6\text{mim}][\text{TF}_2\text{N}]/[C_4\text{mim}][\text{AOT}]$ /benzene microemulsions confirms the larger perturbation in the case of $[C_2\text{mim}][\text{TF}_2\text{N}]/[C_4\text{mim}][\text{AOT}]$ /benzene microemulsions. Here, it is noteworthy to mention that, with the addition of water, we observed significantly larger shifts for the $[C_4\text{mim}][\text{AOT}]$ surfactant signals arising from protons, closer to the headgroup of $[C_4\text{mim}][\text{AOT}]$ compared to that of the long alkyl chains

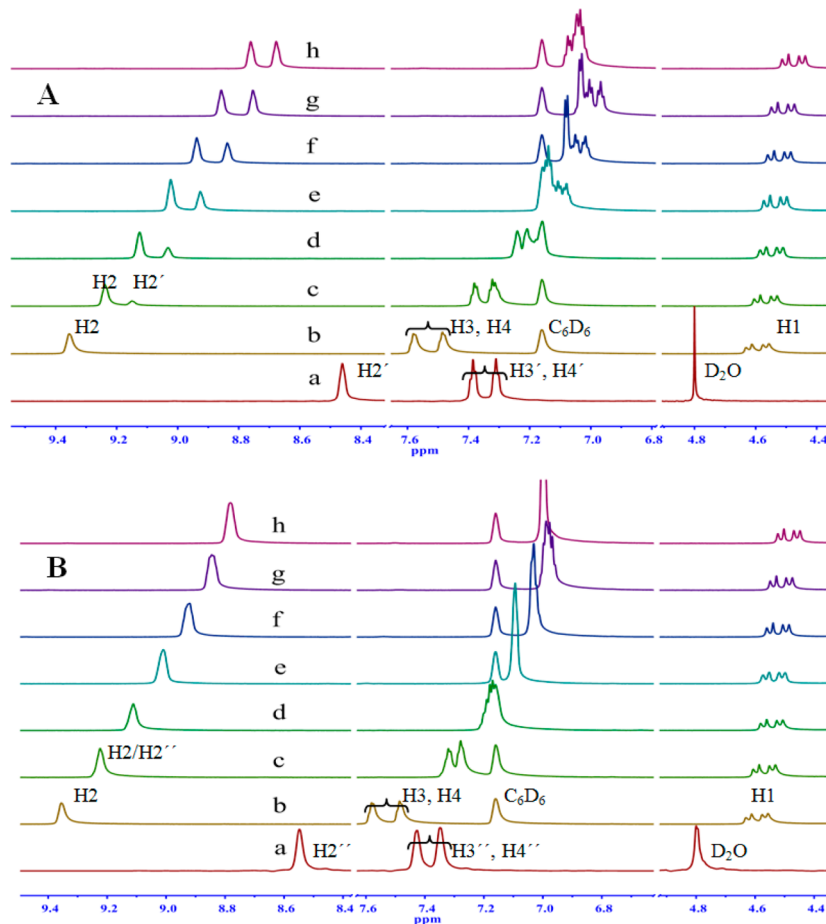


Figure 9. Partial ^1H NMR spectra of (A) neat $[\text{C}_2\text{mim}][\text{TF}_2\text{N}]$ (a), $[\text{C}_2\text{mim}][\text{TF}_2\text{N}]/[\text{C}_4\text{mim}][\text{AOT}]$ /benzene microemulsions at $R = 0$ (b), 0.2 (c), 0.4 (d), 0.6 (e), 0.8 (f), and 1.0 (g), and $[\text{C}_2\text{mim}][\text{TF}_2\text{N}]/[\text{C}_4\text{mim}][\text{AOT}]$ /benzene microemulsions at $R = 1.0$ containing 300 mM of water (h); and (B) neat $[\text{C}_6\text{mim}][\text{TF}_2\text{N}]$ (a), $[\text{C}_6\text{mim}][\text{TF}_2\text{N}]/[\text{C}_4\text{mim}][\text{AOT}]$ /benzene microemulsions at $R = 0$ (b), 0.2 (c), 0.4 (d), 0.6 (e), 0.8 (f), and 1.0 (g), and $[\text{C}_6\text{mim}][\text{TF}_2\text{N}]/[\text{C}_4\text{mim}][\text{AOT}]$ /benzene microemulsions at $R = 1.0$ containing 300 mM of water (h).

(negligible change is observed, Figures S1 and S2 of the Supporting Information). These observations clearly support that the water molecules are located at the interfacial region of the microemulsions.

4. CONCLUSIONS

The study presented here describes the formation and characterization of different IL-in-oil microemulsions containing an anionic surface active ionic liquid (SAIL), $[\text{C}_4\text{mim}][\text{AOT}]$ as a surfactant molecule. To the best of our knowledge, this is the first report of IL-in-oil microemulsions containing SAIL as a surfactant molecule where a comparative study of ionic liquids having alkyl chains of different lengths has been carried out. The work demonstrates that the structural parameters and the interfacial strength of microemulsions can be tuned depending on the nature of the ILs used as the polar phase. The phase behavior study indicates that the area of single phase region increases with an increase in the alkyl chain length of the cation of RTILs and follows the trend $[\text{C}_6\text{mim}][\text{TF}_2\text{N}] > [\text{C}_4\text{mim}][\text{TF}_2\text{N}] > [\text{C}_2\text{mim}][\text{TF}_2\text{N}]$. The strong interaction leading to pronounced penetration and aligning of the cation of $[\text{C}_6\text{mim}][\text{TF}_2\text{N}]$ with the tail part of AOT^- anion makes the interfacial layer more rigid; therefore, the RTIL solubilization capacity increases, and the area of single phase region increases. In the case of ILs where the cationic part is identical and the anionic components are different, the

area of the single phase region follows the trend $[\text{C}_4\text{mim}][\text{TF}_2\text{N}] > [\text{C}_4\text{mim}][\text{PF}_6^-] > [\text{C}_4\text{mim}][\text{BF}_4^-]$. Such a difference in behavior arises due to relatively weak interaction between TF_2N^- anion with C_4mim^+ cation, which causes strong interaction of C_4mim^+ with AOT^- anion, making the interfacial layer more rigid and allowing more RTILs to dissolve inside the polar core of the microemulsions. The difference in strength of interaction is well supported by the ^1H NMR measurements.

The other important finding is that, depending on the IL used, the amount of IL within the core of aggregates in microemulsions can be easily manipulated to directly affect the size of the aggregates. The regular increase in size of aggregates in microemulsions clearly indicates incorporation of ILs in the core of the aggregates. Incorporation of ILs is well supported by entirely different NMR peak positions of ILs inside the reverse micelle compared to neat ILs (vide supra). Furthermore, with the addition of ILs, we observed significantly larger shifts for the $[\text{C}_4\text{mim}][\text{AOT}]$ surfactant signals arising from protons, closer to the headgroup of $[\text{C}_4\text{mim}][\text{AOT}]$ compared to that of the long alkyl chains (negligible change is observed). So, it is evident that ILs interact specifically with the headgroup of the surfactant molecules. The difference in the extent of increase in the size of the aggregates in microemulsions was found to be maximum in the case of $[\text{C}_2\text{mim}][\text{TF}_2\text{N}]/[\text{C}_4\text{mim}][\text{AOT}]$ /benzene microemulsions and follows the trend $[\text{C}_2\text{mim}][\text{TF}_2\text{N}] > [\text{C}_4\text{mim}][\text{TF}_2\text{N}] > [\text{C}_6\text{mim}][\text{TF}_2\text{N}]$. However, the

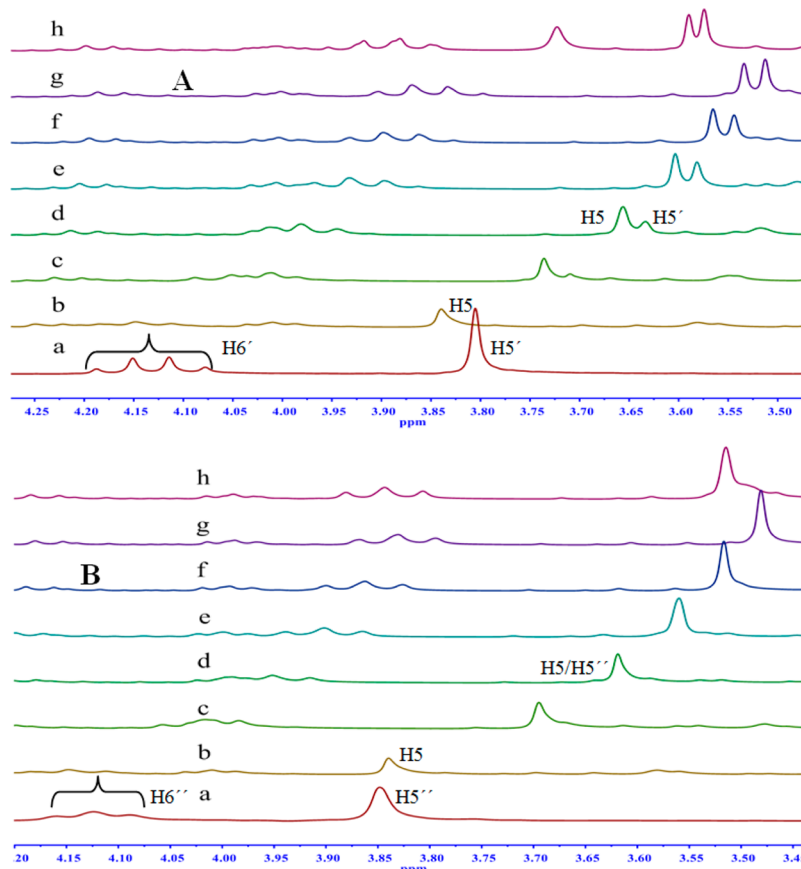


Figure 10. Partial ¹H NMR spectra showing variation of H5'/H5'' and H6'/H6'' with (A) neat [C₂mim][TF₂N] (a), [C₂mim][TF₂N]/[C₄mim][AOT]/benzene microemulsions at $R = 0$ (b), 0.2 (c), 0.4 (d), 0.6 (e), 0.8 (f), and 1.0 (g), and [C₂mim][TF₂N]/[C₄mim][AOT]/benzene microemulsions at $R = 1.0$ containing 300 mM of water (h); and (B) neat [C₆mim][TF₂N] (a), [C₆mim][TF₂N]/[C₄mim][AOT]/benzene microemulsions at $R = 0$ (b), 0.2 (c), 0.4 (d), 0.6 (e), 0.8 (f), and 1.0 (g), and [C₆mim][TF₂N]/[C₄mim][AOT]/benzene microemulsions at $R = 1.0$ containing 300 mM of water (h).

size increase was almost the same with an increase in R value in the case of ILs with different anions. The observed differences have been explained by considering the rigidity of the respective microemulsions (*vide supra*).

The studied effect of temperature on the behavior of different microemulsions further opens up the possibility of application of microemulsions at high temperature. In all the cases, the size of aggregates in microemulsions decreases with increasing temperature. The extent of decrease in size is different in the case of ILs having different alkyl chains, which arises due to the difference in the rigidity of the microemulsions (*vide supra*). Contrary to this, the extent of decrease in size is almost the same in the case of ILs having different anions. Once again, the observed uniform decrease in size arises due to similar rigidity of microemulsions having ILs with different anions.

Most importantly, the effects of water addition on microemulsions containing hydrophobic ILs were reported for the first time. The addition of water causes a huge change in the microstructure of the IL microemulsions. The maximum increase in size with the addition of water (final concentration of water was 300 mM) was observed for [C₂mim][TF₂N]/[C₄mim][AOT]/benzene microemulsions and follows the trend [C₂mim][TF₂N] > [C₄mim][TF₂N] > [C₆mim][TF₂N]. The observed difference arises due to the decrease in curvature parameter (*vide supra*), which is maximum in the case of [C₂mim][TF₂N]/[C₄mim][AOT]/benzene microemulsions. Water molecules being insoluble in [C_nmim][TF₂N] ILs are

inclined to occupy the interfacial layers of the microemulsions and replace some of the [C_nmim]⁺ cation and decrease the curvature of the surfactant. The maximum perturbation of surfactant headgroup area was observed with the addition of water to [C₂mim][TF₂N]/[C₄mim][AOT]/benzene microemulsions. This observation was supported by the proton-NMR spectra (*vide supra*). Also, with the addition of water we observed significantly larger shifts for the [C₄mim][AOT] surfactant signals arising from protons, closer to the headgroup of [C₄mim][AOT] compared to that of the longer alkyl chains (negligible change is observed), which provides a clear picture about the location of the added water molecule.

The effect of water addition in different microemulsions containing ILs of different hydrophobicity (hydrophobicity trend; [C₄mim][TF₂N] > [C₄mim][PF₆] > [C₄mim][BF₄]) provides many other important information (*vide supra*). The increase in size of aggregates in microemulsions with the addition of water follow exactly the same trend as the hydrophobicity of the IL (*vide supra*).

In summary, our study clearly provides different ways to tune the structure of microemulsions, which in turn can provide different routes to alter the size of the nanoparticles/polymers and provided volume for performing organic reactions. Moreover, the ability of the designed microemulsions to dissolve a wide variety of ionic liquids (hydrophobic, hydrophilic, protic, and hydrolysis-stable TF₂N⁻ anion)⁷¹

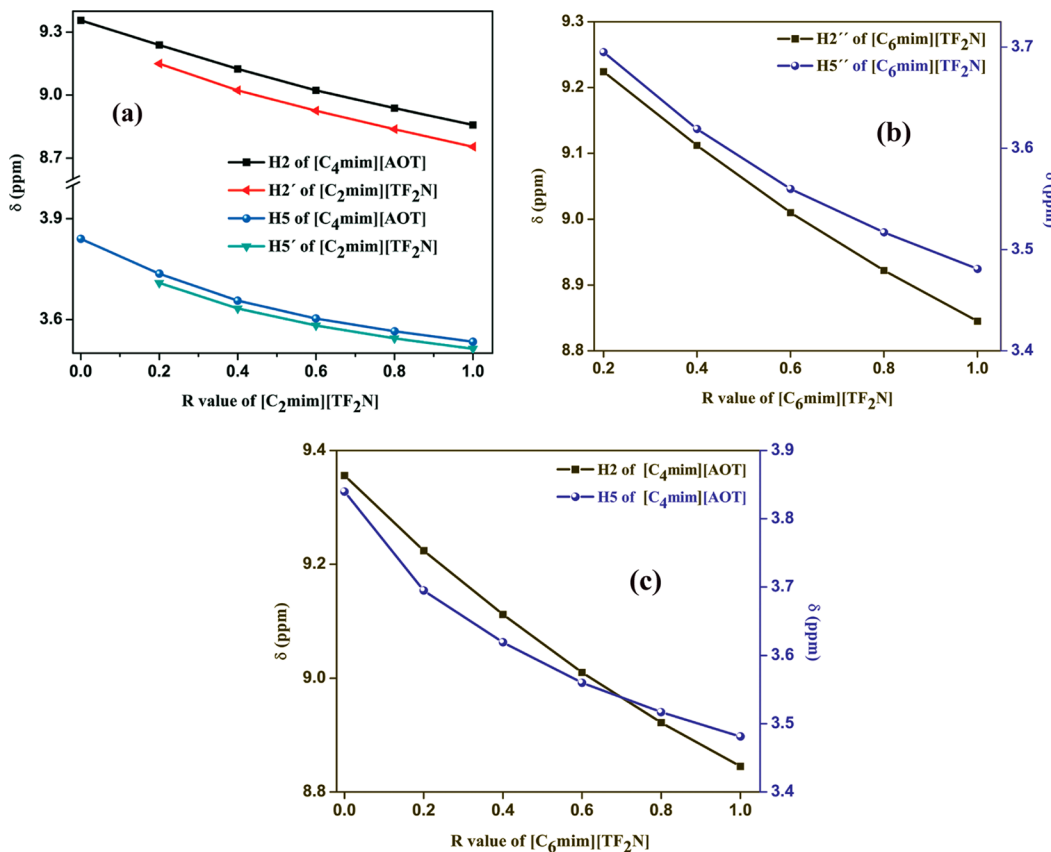


Figure 11. Variation of ¹H chemical shifts of (a) H2 and H5 of [C₄mim][AOT] and H2' and H5' of [C₂mim][TF₂N] in [C₂mim][TF₂N]/[C₄mim][AOT]/benzene microemulsions with increasing R value of [C₂mim][TF₂N]; (b) H2'' and H5'' of [C₆mim][TF₂N] and (c) H2 and H5 of [C₄mim][AOT] in [C₆mim][TF₂N]/[C₄mim][AOT]/benzene microemulsions with increasing R value of [C₆mim][TF₂N].

containing ionic liquids) coupled with their high temperature stability can be utilized for different fields of interest.

■ ASSOCIATED CONTENT

Supporting Information

Proton-NMR spectra and phase boundaries data of the RTILs/[C₄mim][AOT]/benzene ternary systems. This material is available free of charge via the Internet at <http://pubs.acs.org>.

■ AUTHOR INFORMATION

Corresponding Author

*E-mail: nilmoni@chem.iitkgp.ernet.in. Fax: 91-3222-255303.

Notes

The authors declare no competing financial interest.

■ ACKNOWLEDGMENTS

N.S. thanks the Council of Scientific and Industrial Research (CSIR) and Government of India, for generous research grants. V.G.R., S.M., and S.G. are thankful to CSIR, and C.B. is thankful to UGC for a research fellowship. We are thankful to DST FIST for funding the NMR equipment.

■ REFERENCES

- (1) Dwars, T.; Paetzold, E.; Oehme, G. *Angew. Chem.* **2005**, *117*, 7338–7364.
- (2) Crans, D. C.; Trujillo, A. M.; Bonetti, S.; Rithner, C. D.; Baruah, B.; Levinger, N. E. *J. Org. Chem.* **2008**, *73*, 9633–9640.
- (3) Eastoe, J.; Gold, S.; Rogers, S. E.; Wyatt, P.; Steytler, D. C.; Gurgel, A.; Heenan, R. K.; Fan, X.; Beckman, E. J.; Enick, R. M. *Angew. Chem., Int. Ed.* **2006**, *45*, 3675–3677.
- (4) Liu, Y.; Jessop, P. G.; Cunningham, M.; Eckert, C. A.; Liotta, C. L. *Science* **2006**, *313*, 958–960.
- (5) Wagner, G. W.; Procell, L. R.; Yang, Y.-C.; Bunton, C. A. *Langmuir* **2001**, *17*, 4809–4811.
- (6) Bonini, M.; Bardi, U.; Berti, D.; Neto, C.; Baglioni, P. *J. Phys. Chem. B* **2002**, *106*, 6178–6183.
- (7) Lv, F. F.; Zheng, L. Q.; Tung, C. *Int. J. Pharm.* **2005**, *301*, 237–246.
- (8) Altamirano, M. S.; Borsarelli, C. D.; Cosa, J. J.; Previtali, C. M. *J. Colloid Interface Sci.* **1998**, *205*, 390–396.
- (9) Hasegawa, M.; Sugimura, T.; Suzuki, Y.; Kitahara, A. *J. Phys. Chem.* **1994**, *98*, 2120–2124.
- (10) Correa, N. M.; Biasutti, M. A.; Silber, J. J. *J. Colloid Interface Sci.* **1996**, *184*, 570–578.
- (11) Sedgwick, M.; Cole, R. L.; Rithner, C. D.; Crans, D. C.; Levinger, N. E. *J. Am. Chem. Soc.* **2012**, *134*, 11904–11907.
- (12) Riter, R. E.; Undiks, E. P.; Levinger, N. E. *J. Am. Chem. Soc.* **1998**, *120*, 6062–6067.
- (13) Fathi, H.; Kelly, J. P.; Vasquez, V. R.; Graeve, O. A. *Langmuir* **2012**, *28*, 9267–9274.
- (14) Horn, W. D. V.; Ogilvie, M. E.; Flynn, P. F. *J. Am. Chem. Soc.* **2009**, *131*, 8030–8039.
- (15) Biswas, R.; Chakraborti, T.; Bagchi, B.; Ayappa, K. G. *J. Chem. Phys.* **2012**, *137*, 014515–014523.
- (16) Bagchi, B. *Chem. Rev.* **2005**, *105*, 3197–3219.
- (17) Mandal, D.; Datta, A.; Pal, S. K.; Bhattacharyya, K. *J. Phys. Chem. B* **1998**, *102*, 9070–9073.
- (18) Dutta, P.; Sen, P.; Mukherjee, S.; Halder, A.; Bhattacharyya, K. *J. Phys. Chem. B* **2003**, *107*, 10815–10822.

- (19) Agazzi, F. M.; Falcone, R. D.; Silber, J. J.; Correa, N. M. *J. Phys. Chem. B* **2011**, *115*, 12076–12084.
- (20) Nave, S.; Eastoe, J.; Heenan, R. K.; Steytler, D.; Grillo, I. *Langmuir* **2000**, *16*, 8741–8748.
- (21) Angelico, R.; Ceglie, A.; Colafemmina, G.; Delfine, F.; Olsson, U.; Palazzo, G. *Langmuir* **2004**, *20*, 619–631.
- (22) Piletic, I. R.; Moilanen, D. E.; Levinger, N. E.; Fayer, M. D. *J. Am. Chem. Soc.* **2006**, *128*, 10366–10367.
- (23) Baruah, B.; Roden, J. M.; Sedgwick, M.; Correa, N. M.; Crans, D. C.; Levinger, N. E. *J. Am. Chem. Soc.* **2006**, *128*, 12758–12765.
- (24) Das, K. P.; Ceglie, A.; Lindman, B. *J. Phys. Chem.* **1987**, *91*, 2938–2946.
- (25) Ray, S.; Moulik, S. P. *Langmuir* **1994**, *10*, 2511–2515.
- (26) Shirota, H.; Horie, K. *J. Phys. Chem. B* **1999**, *103*, 1437–1443.
- (27) Shirota, H.; Segawa, H. *Langmuir* **2004**, *20*, 329–335.
- (28) Riter, R. E.; Kimmel, J. R.; Undiks, E. P.; Levinger, N. E. *J. Phys. Chem. B* **1997**, *101*, 8292–8297.
- (29) Novaira, M.; Moyano, F.; Biasutti, M. A.; Silber, J. J.; Correa, N. M. *Langmuir* **2008**, *24*, 4637–4646.
- (30) Silber, J. J.; Falcone, R. D.; Correa, N. M.; Biasutti, M. A.; Abuin, E.; Lissi, E.; Campodonico, P. *Langmuir* **2003**, *19*, 2067–2071.
- (31) Lü, H. H.; An, X. Q.; Shen, W. G. *J. Chem. Eng. Data* **2008**, *53*, 727–731.
- (32) Liu, L. P.; Bauduin, P.; Zemb, T.; Eastoe, J.; Hao, J. C. *Langmuir* **2009**, *25*, 2055–2059.
- (33) Rojas, O.; Koetz, J.; Kosmella, S.; Tiersch, B.; Wacker, P.; Kramer, M. *J. Colloid Interface Sci.* **2009**, *333*, 782–790.
- (34) Ranke, J.; Stolte, S.; Stormann, R.; Arning, J.; Jastorff, B. *Chem. Rev.* **2007**, *107*, 2183–2206.
- (35) Wei, J.; Su, B.; Yang, J.; Xing, H.; Bao, Z.; Yang, Y.; Ren, Q. *J. Chem. Eng. Data* **2011**, *S6*, 3698–3702.
- (36) Wei, J.; Su, B.; Xing, H.; Bao, Z.; Yang, Y.; Ren, Q. *Colloids Surf., A* **2012**, *396*, 213–218.
- (37) Wei, J.; Su, B.; Liang, R.; Xing, H.; Bao, Z.; Yang, Y.; Ren, Q. *J. Chem. Eng. Data* **2012**, *57*, 1274–1278.
- (38) Gao, Y.; Li, N.; Zheng, L.; Zhao, X.; Zhang, J.; Cao, Q.; Zhao, M.; Li, Z.; Zhang, G. *Chem.—Eur. J.* **2007**, *13*, 2661–2670.
- (39) Li, N.; Cao, Q.; Gao, Y. A.; Zhang, J.; Zheng, L. Q.; Bai, X. T.; Dong, B.; Li, Z.; Zhao, M. W.; Yu, L. *ChemPhysChem* **2007**, *8*, 2211–2217.
- (40) Gao, Y.; Li, N.; Zheng, L.; Bai, X.; Yu, L.; Zhao, X.; Zhang, J.; Zhao, M.; Li, Z. *J. Phys. Chem. B* **2007**, *111*, 2506–2513.
- (41) Gao, H. X.; Li, J. C.; Han, B. X.; Chen, W. N.; Zhang, J. L.; Zhang, R.; Yan, D. D. *Phys. Chem. Chem. Phys.* **2004**, *6*, 2914–2916.
- (42) Eastoe, J.; Gold, S.; Rogers, S. E.; Paul, A.; Welton, T.; Heenan, R. K.; Grillo, I. *J. Am. Chem. Soc.* **2005**, *127*, 7302–7303.
- (43) Gao, Y. N.; Wang, S. Q.; Zheng, L. Q.; Han, S. B.; Zhang, X.; Lu, D. M.; Yu, L.; Ji, Y. Q.; Zhang, G. Y. *J. Colloid Interface Sci.* **2006**, *301*, 612–616.
- (44) Gao, Y. A.; Zhang, J.; Xu, H. Y.; Zhao, X. Y.; Zheng, L. Q.; Li, X. W.; Yu, L. *ChemPhysChem* **2006**, *7*, 1554–1561.
- (45) Li, N.; Gao, Y. A.; Zheng, L. Q.; Zhang, J.; Yu, L.; Li, X. W. *Langmuir* **2007**, *23*, 1091–1097.
- (46) Gao, Y. A.; Li, N.; Zheng, L. Q.; Bai, X. T.; Yu, L.; Zhao, X. Y.; Zhang, J.; Zhao, M. W.; Li, Z. *J. Phys. Chem. B* **2007**, *111*, 2506–2513.
- (47) Falcone, R. D.; Correa, N. M.; Silber, J. J. *Langmuir* **2009**, *25*, 10426–10429.
- (48) Qiu, Z. M.; Texter, J. *Curr. Opin. Colloid Interface Sci.* **2008**, *13*, 252–262.
- (49) Sando, G. M.; Dahl, K.; Owrusky, J. C. *Chem. Phys. Lett.* **2006**, *418*, 402–407.
- (50) Li, J. C.; Zhang, J. L.; Han, B. X.; Wang, Y.; Gao, L. *J. Chem. Phys.* **2004**, *121*, 7408–7412.
- (51) Chakrabarty, D.; Seth, D.; Chakraborty, A.; Sarkar, N. *J. Phys. Chem. B* **2005**, *109*, 5753–5758.
- (52) Gao, Y.; Li, N.; Zheng, L. Q.; Zhao, X. Y.; Zhang, J.; Cao, Q.; Zhao, M. W.; Li, Z.; Zhang, G. Y. *Chem.—Eur. J.* **2007**, *13*, 2661–2670.
- (53) Liu, J. H.; Cheng, S. Q.; Zhang, J. L.; Feng, X. Y.; Fu, X. G.; Han, B. X. *Angew. Chem., Int. Ed.* **2007**, *46*, 3313–3315.
- (54) Gao, Y. N.; Li, N.; Hilfert, L.; Zhang, S. H.; Zheng, L. Q.; Yu, L. *Langmuir* **2009**, *25*, 1360–1365.
- (55) Moniruzzaman, M.; Kamiya, N.; Goto, M. *J. Colloid Interface Sci.* **2010**, *352*, 136–142.
- (56) Moniruzzaman, M.; Tahara, Y.; Tamura, M.; Kamiya, N.; Goto, M. *Chem. Commun.* **2010**, 1452–1454.
- (57) Falcone, R. D.; Baruah, B.; Gaidamauskas, E.; Rithner, C. D.; Correa, N. M.; Silber, J. J.; Crans, D. C.; Levinger, N. E. *Chem.—Eur. J.* **2011**, *17*, 6837–6846.
- (58) Pramanik, R.; Ghatak, C.; Rao, V. G.; Sarkar, S.; Sarkar, N. *J. Phys. Chem. B* **2011**, *115*, 5971–5979.
- (59) Pramanik, R.; Sarkar, S.; Ghatak, C.; Rao, V. G.; Sarkar, N. *Chem. Phys. Lett.* **2011**, *512*, 217–222.
- (60) Zech, O.; Thomaier, S.; Bauduin, P.; Rück, T.; Touraud, D.; Kunz, W. *J. Phys. Chem. B* **2009**, *113*, 465–473.
- (61) Zech, O.; Thomaier, S.; Kolodziejski, A.; Touraud, D.; Grillo, I.; Kunz, W. *Chem.—Eur. J.* **2010**, *16*, 783–786.
- (62) El Seoud, O. A.; Pires, P. A. R.; Abdel-Moghny, T.; Bastos, E. L. *J. Colloid Interface Sci.* **2007**, *313*, 296–304.
- (63) Galgano, P. D.; El Seoud, O. A. *J. Colloid Interface Sci.* **2010**, *345*, 1–11.
- (64) Ferreyra, D. D.; Correa, N. M.; Silber, J. J.; Falcone, R. D. *Phys. Chem. Chem. Phys.* **2012**, *14*, 3460–3470.
- (65) Inoue, T.; Dong, B.; Zheng, L. Q. *J. Colloid Interface Sci.* **2007**, *307*, 578–581.
- (66) Cheng, S.; Zhang, J.; Zhang, Z.; Han, B. *Chem. Commun.* **2007**, 2497–2499.
- (67) Rabe, C.; Koetz, J. *Colloids Surf., A* **2010**, *354*, 261–267.
- (68) Rao, V. G.; Ghosh, S.; Ghatak, C.; Mandal, S.; Brahmachari, U.; Sarkar, N. *J. Phys. Chem. B* **2012**, *116*, 2850–2855.
- (69) Rao, V. G.; Mandal, S.; Ghosh, S.; Banerjee, C.; Sarkar, N. *J. Phys. Chem. B* **2012**, *116*, 8210–8221.
- (70) Freire, M. G.; Santos, L. M. N. B. F.; Fernandes, A. M.; Coutinho, J. A. P.; Marrucho, I. M. *Fluid Phase Equilib.* **2007**, *261*, 449–454.
- (71) Porada, J. H.; Mansuetto, M.; Laschat, S.; Stubenrauch, C. *Soft Matter* **2011**, *7*, 6805–6810.
- (72) Shi, W.; Maginn, E. J. *J. Phys. Chem. B* **2008**, *112*, 2045–2055.
- (73) Kerle, D.; Ludwig, R.; Geiger, A.; Paschek, D. *J. Phys. Chem. B* **2009**, *113*, 12727–12735.
- (74) Karadas, F.; Atilhan, M.; Aparicio, S. *Energy Fuels* **2010**, *24*, 5817–5828.
- (75) Cadena, C.; Anthony, J. L.; Shah, J. K.; Morrow, T. I.; Brennecke, J. F.; Maginn, E. J. *J. Am. Chem. Soc.* **2004**, *126*, 5300–5308.
- (76) Maginn, E. J. *Acc. Chem. Res.* **2007**, *40*, 1200–1207.
- (77) Kelkar, M. S.; Maginn, E. J. *J. Phys. Chem. B* **2007**, *111*, 4867–4876.
- (78) Santos, L. M. N. B. F.; Lopes, J. N. C.; Coutinho, J. A. P.; Esperancia, J. M. S. S.; Gomes, L. R.; Marrucho, I. M.; Rebelo, L. P. N. *J. Am. Chem. Soc.* **2007**, *129*, 284–285.
- (79) Lopes, J. N. C.; Pádua, A. A. H. *J. Phys. Chem. B* **2004**, *108*, 16893–16898.
- (80) Lopes, J. N. C.; Shimizu, K.; Pádua, A. A. H.; Umebayashi, Y.; Fukuda, S.; Fujii, K.; Ishiguro, S. I. *J. Phys. Chem. B* **2008**, *112*, 9449–9455.
- (81) Bini, R.; Bortolini, O.; Chiappe, C.; Pieraccini, D.; Siciliano, T. *J. Phys. Chem. B* **2007**, *111*, 598–604.
- (82) Pramanik, R.; Sarkar, S.; Ghatak, C.; Rao, V. G.; Sarkar, N. *J. Phys. Chem. B* **2011**, *115*, 2322–2330.
- (83) Gao, Y.; Han, S.; Han, B.; Li, G.; Shen, D.; Li, Z.; Du, J.; Hou, W.; Zhang, G. *Langmuir* **2005**, *21*, 5681–5684.
- (84) Liu, D.; Ma, J.; Cheng, H.; Zhao, Z. *Colloids Surf., A* **1998**, *135*, 157–164.
- (85) Headley, A. D.; Jackson, N. M. *J. Phys. Org. Chem.* **2002**, *15*, 52–55.